The advantage of the electrochemical redox process between IP and $IP^{\bullet+}$ in nonaqueous medium over that in aqueous medium for practical purpose is reasonably understood.

Registry No. BBB, 74-31-7; BBB·2HBF$_4$, 119393-41-8; BQB, 6246-98-6; lithium tetrafluoroborate, 14283-07-9; polyaniline, 25233-30-1.

References and Notes

(1) Paul, E. W.; Ricco, A. J.; Wrighton, M. S. *J. Phys. Chem.* **1985**, *89*, 1441.
(2) Kitani, A.; Yano, J.; Sasaki, K. *J. Electroanal. Chem.* **1986**, *209*, 227.
(3) Kaneko, M.; Nakamura, H. *J. Chem. Soc., Chem. Commun.* **1985**, 346.
(4) Enomoto, T.; Allen, D. P. *Bridgestone News Release* **1987**, Sept 9. Address of T. Enomoto: International Public Relations, Bridgestone Corporation, 1-10-1, Kyobashi, Chuo-ku, Tokyo 104, Japan.
(5) *Chem. Week* **1987**, Oct 14, 40.
(6) Furukawa, Y.; Ueda, F.; Hyodo, Y.; Harada, I.; Nakajima, T.; Kawagoe, T. *Macromolecules* **1988**, *21*, 1297.
(7) This compound is also called *N,N'*-diphenyl-*p*-phenylenediamine (DPPD) and *N,N'*-diphenyl-*p*-benzoquinone diamine (QDA).
(8) This compound is also called *N,N'*-diphenyl-*p*-quinone diimine (DPQI) and *N,N'*-diphenyl-*p*-benzoquinone diimine (QDI).
(9) Honzl, J.; Metalová, M. *Tetrahedron* **1969**, *25*, 3641.
(10) Linschitz, H.; Rennert, J.; Korn, T. M. *J. Am. Chem. Soc.* **1954**, *76*, 5839.
(11) Hagiwara, T.; Demura, T.; Iwata, K. *Synth. Met.* **1987**, *18*, 317.
(12) Nakajima, T.; Toyosawa, S.; Suzuki, K.; Miyazaki, T.; Kitamura, T.; Kawagoe, T. Japan Patent Pub. 62-149724, 1987.
(13) Linschitz, H.; Ottolenghi, M.; Bensasson, R. *J. Am. Chem. Soc.* **1967**, *89*, 4592.
(14) Ohsawa, T.; Kabata, O.; Kimura, O.; Yoshino, K. reported in the International Conference on Science and Technology of Synthetic Metals, June 26–July 2, 1988, Santa Fe and: *Synth. Met.*, in press.
(15) Salaneck, W. R.; Lundström, I.; Hjertberg, T.; Duke, C. B.; Conwell, E.; Paton, A.; MacDiarmid, A. G.; Somasiri, N. L. D.; Huang, W. S.; Richter, A. F. *Synth. Met.* **1987**, *18*, 291.
(16) Snauwaert, P.; Lazzaroni, R.; Riga, J.; Verbist, J. J. *Synth. Met.* **1987**, *18*, 335.
(17) Palmer, M. H.; Moyes, W.; Spiers, M.; Ridyard, J. N. A. *J. Mol. Struct.* **1979**, *53*, 235.
(18) Stafström, S.; Brédas, J. L.; Epstein, A. J.; Woo, H. S.; Tanner, D. B.; Huang, W. S.; MacDiarmid, A. G. *Phys. Rev. Lett.* **1987**, *59*, 1464.
(19) Okabayashi, K.; Hyodo, S. *Proceedings of the 54th Spring Meeting of the Chemical Society of Japan*; Tokyo, 1987; p 124.
(20) MacDiarmid, A. G.; Chiang, J. C.; Richter, A. F.; Epstein, A. J. *Synth. Met.* **1987**, *18*, 285.
(21) Furukawa, Y.; Hara, T.; Hyodo, Y.; Harada, I. *Synth. Met.* **1986**, *16*, 189.

Investigation of Diffusion in Polystyrene Using Secondary Ion Mass Spectroscopy

S. J. Whitlow and R. P. Wool*

Department of Materials Science and Engineering, University of Illinois, 1304 W. Green Street, Urbana, Illinois 61801.

Received August 8, 1988; Revised Manuscript Received November 22, 1988

ABSTRACT: SIMS is an ideal tool for examining polymer diffusion because it combines excellent depth resolution with direct depth profile measurement. This is a preliminary study on the use of SIMS for measuring depth profiles of polymers. Bilayer samples composed of $\bar{M}_w$ = 111 000/93 000 deuterated–protonated monodisperse polystyrene films were chosen for this investigation. The deuterated film was ≈1000 Å thick and the protonated film was ≈2500 Å thick. Before testing, samples were covered with 200 Å of Au to prevent charging. Analysis of a sharp interface showed a depth resolution of 138 Å, significantly better than that of several other methods. The depth profile was measured for a bilayer after annealing at 125 °C for 14 400 s. The diffused profile was analyzed by using the Grube method and the self-diffusion coefficient, $\tilde{D}$, was found to be 5.6×10^{-16} cm^2/s.

Introduction

Understanding polymer diffusion is important for controlling mechanical properties of melt-processed polymer blends and welded polymers. Recent techniques used to study polymer melt diffusion include forward recoil spectroscopy[1,2] (FRES), IR spectroscopy,[3,4] photobleaching,[5] and small-angle neutron scattering (SANS).[6,7] This paper presents a new approach for measuring polymer diffusion, namely, the application of secondary ion mass spectroscopy (SIMS). Like the above methods, SIMS is sensitive to both hydrogen and deuterium which makes it useful for tracer studies. The primary advantages of SIMS are that it has excellent depth resolution and it is able to directly measure a concentration profile. Also, this technique can monitor elements to much greater depths than some of the above methods.

SIMS has long been an important tool for the analysis of semiconductors but little work has been done on polymers. Most SIMS applications used the static (low-energy primary beam) mode to characterize polymer surfaces by their mass spectra.[8,9] Relatively little work has been done on depth profiling of polymers[10,11] with no quantitative analysis. This paper will present a quantitative analysis of diffusion in a deuterated–protonated polystyrene bilayer system.

SIMS

The basis for SIMS is the ejection of charged atoms and molecules caused by an impinging ion beam. The incoming primary ion transfers energy and momentum to the region around the point of impact. One result of this event is loss of surface material by sputtering.[12] A second result is changes in the target structure known as atomic mixing.[13]

The sputtering process is shown schematically in Figure 1. The incoming primary ion dissipates a large portion of its energy in the region near the surface. The average distance a primary ion penetrates the sample is known as the primary ion range. This parameter characterizes the

0024-9297/89/2222-2648$01.50/0

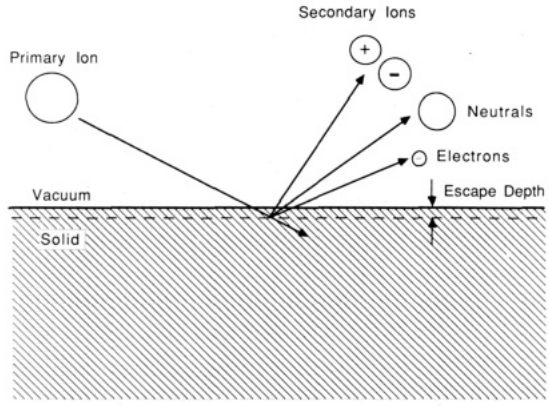

Figure 1. Schematic of the sputtering process caused by an impinging primary ion.

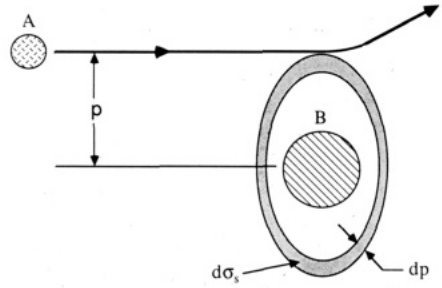

Figure 2. Impact parameter, p, is the distance of closest approach between incoming atom A and target atom B. The differential cross section, $d\sigma_s$, is the area a trajectory of A must pass to impart a given energy to B.

distribution of depths where primary ions lose all of their energy. This range depends on several factors, including primary ion accelerating voltage and the masses of the primary ion and target. Target atoms within a certain (escape) depth have enough kinetic energy to overcome the surface potential and eject from the sample. The escape depth depends on the target material and is always smaller than the primary ion range. Most sputtered species are neutral, although a small number undergo charge exchange with their local environment which result in conversion to positive and negative secondary ions.[14] The surface composition can be determined by analyzing the secondary ions with a mass spectrometer.

Sputtered particles may be atoms or clusters of atoms. The number and type of clusters increase with a decrease in primary ion current density. This fact has been used to characterize polymer surfaces by using the static SIMS mode. For primary current densities in the dynamic SIMS mode ($\geq$10 nA/cm^2) sputtering causes erosion of the sample surface. Repeated exposure of the target to the beam can be used to monitor an element as a function of depth. The secondary ion current can be converted to an atomic concentration with the use of standards. In the present study with deuterated–protonated polymers only relative differences in concentration are important. Therefore, it is not necessary to convert the secondary ion current to an absolute concentration.

Besides sputtering, ion bombardment also produces atomic mixing. The two principal contributions to atomic mixing are recoil implantation and cascade mixing. For a given primary ion energy, the energy transferred from the primary ion to the target atom depends on the distance of closest approach, p, known as the impact parameter (Figure 2). For atoms of comparable mass, recoil implantation will occur when the impact parameter is small. The collision is similar to that between two billiard balls. The primary ion will elastically transfer a significant

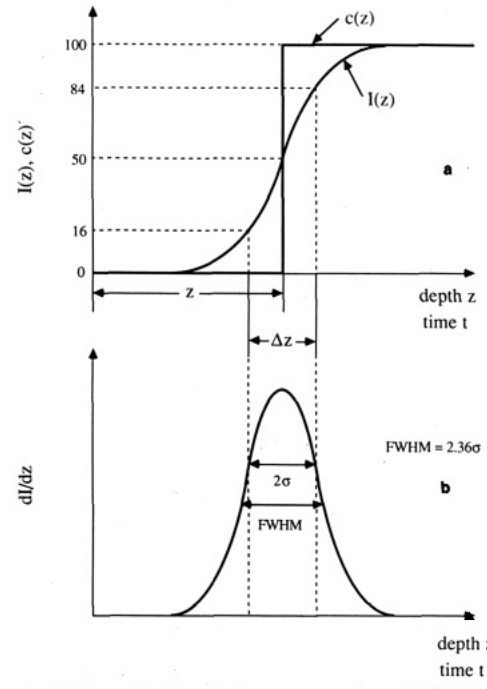

Figure 3. (a) Broadening of the measured profile, $I(z)$, relative to the initial step profile, $c(z)$, is quantified by the depth resolution Δz. The measured profile, $I(z)$, is a convolution of the true profile and the response function (b). In most cases, the response function is the negative derivative of the measured profile.[12]

portion of its energy and momentum. As a result, the target atom will recoil deep into the sample.

Large impact parameter collisions produce cascade mixing. Less energy is transferred to the target atom because the interaction between the ion and target atom now involves a screened Coulombic potential instead of the hard-sphere potential used for recoil implantation. Instead of recoiling into the sample, the target atom displaces its neighboring atoms producing secondary cascades. There is a general homogenization of all the near-surface region atoms affected by the cascade. The thickness of the affected region is usually on the order of the primary ion range in the sample.[13]

The probability for transferring a given amount of energy is usually expressed in terms of the area through which the ion trajectory must pass if energy transfer is to occur (Figure 2).[15] This area is called the differential cross section, $d\sigma_s$. In terms of the impact parameter, the differential cross section is given as

$$d\sigma_s = 2\pi p\, dp$$

Obviously, the probability for energy transfer increases with increasing impact parameter. Consequently, cascade mixing will be more probable than recoil implantation and will be the dominant contribution to atomic mixing.

Cascade mixing has the adverse effect of broadening the measured profile of an initially sharp interface (Figure 3a). The ideally sharp interface is given by the step function $c(z)$. The measured profile is given by the secondary ion current, $I(z)$, which is measured as a function of time during the experiment. Because sputtering rates vary from target to target, in situ depth measurements are extremely difficult. After testing, the time scale is converted to a distance scale by measuring the depth of the sputtered crater.

Broadening of a measured profile is quantified by the depth resolution, Δz (Figure 3a). This parameter is defined as the interval where the measured current intensity drops by a certain amount.[12,13] There are several definitions of

Δz, but the most common is the depth range where the signal drops from 84% to 16% of the maximum secondary ion current. This is an arbitrary definition that corresponds to twice the standard deviation of the resolution or response function (Figure 3b). The resolution function is the negative derivative of the measured profile and is assumed to be Gaussian.

The optimal depth of resolution is determined by the cascade mixing range.[13] The depth of cascade mixing will depend on the primary ion energy, the atomic numbers of the primary ion and target, and the angle between the primary beam and sample surface. Low energy, high atomic number ions at small ion beam to sample surface angles can be used to minimize cascade mixing.

The optimal Δz can be severely degraded by several factors including instrument parameters, nonuniform sputtering, and initial sample topography. The effects of instrument parameters depend on the particular SIMS being utilized. These parameters are always minimized before testing. Nonuniform sputtering is a problem only for multielemental targets whose components have significantly different sputter yields. Fortunately, nonuniform sputtering is not an issue for the polymers used in this experiment. On the other hand, care must be taken to make sure that the sample is flat. On a rough surface, a uniform sputtering rate will produce signals simultaneously from different depths, hence degrading the depth resolution.

Even with a judicious choice of instrument settings and careful sample preparation there is still one difficulty to overcome. Polymers are insulators and they charge when bombarded with ions. Secondary electrons lost during sputtering leave a net positive charge in the specimen[13] which has a detrimental effect on primary ion–sample interactions as well as the secondary ion–sample interactions. Several approaches have been used to solve this problem,[14] including gold coating and the use of grids and masks that supply electrons to the sputtered region during testing. Another approach is to change the sample surface potential during data acquisition, but this approach can be quite difficult. Gold coating was used in this study as described below.

Experimental Methods

Polymer Samples. Samples for this experiment consisted of bilayers of deuterated and protonated polystyrene films. The protonated polystyrene (HPS), from Pressure Chemical Co., had a weight-average molecular weight of $\bar{M}_w$ = 93 000 and a polydispersity index of 1.06. Fully deuterated polystyrene (DPS), obtained from Polymer Laboratories, had $\bar{M}_w$ = 111 000 and a polydispersity index of 1.05. Solutions of each polymer were made with reagent grade toluene. Concentrations for the HPS and DPS solutions were 0.03 and 0.01 g/mL, respectively.

HPS Layer Preparation. Silicon substrates of approximately 1.8 cm × 0.8 cm were cut from a large wafer. The substrates were cleaned in filtered toluene and allowed to air dry. Then 45 mL of HPS solution was filtered into a graduated cylinder. The HPS layer was solution cast onto the silicon by placing the substrate into the graduated cylinder for a fixed length of time. A variable-speed motor, set at 20 rpm, was employed to dip and remove samples from the solution at a constant rate. Once a number of films were cast they were dried for 1 week in a vacuum oven at room temperature. HPS films for this experiment were found to be about 2500 Å thick.

DPS Layer Preparation. Microscope glass slides were cut into 1.5 cm × 1.5 cm squares and cleaned with deionized water. The squares were individually spun dry on a photoresist spinner and a nitrogen jet was used to remove any water that had been trapped between the slide and the spindle. The dry slide was placed back onto the photoresist spinner. Approximately 30 μm of filtered DPS solution was placed on the center of the slide. The square was then spun at 2000 rpm for 40 s. This procedure produced DPS films of about 1000-Å thickness.

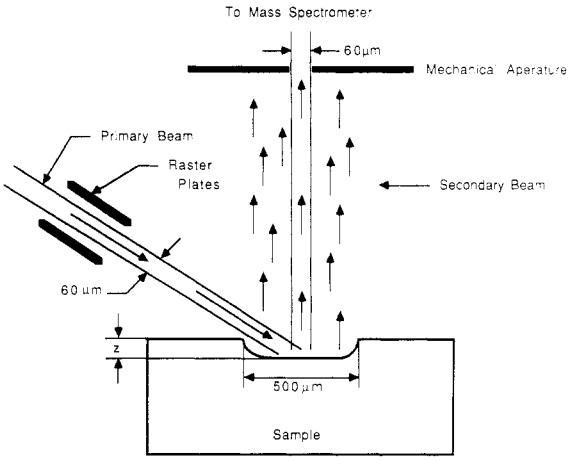

Figure 4. Schematic for the SIMS testing configuration.

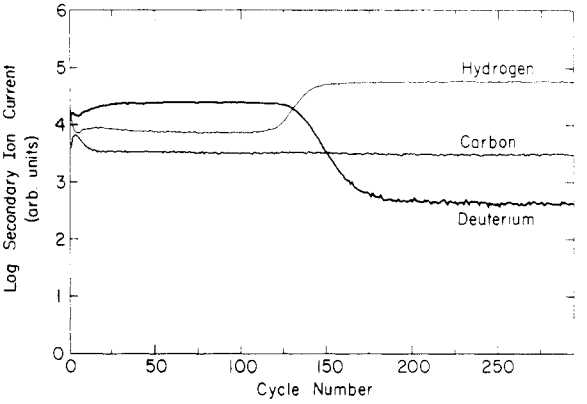

Figure 5. Raw concentration profile. The abscissa is by channels (or cycles) where each channel represents 3 s. Each element is monitored for 1 s and with three elements; each channel (or cycle) takes 3 s to complete.

Bilayer Preparation. The DPS film was floated from the glass slide onto the surface of deionized water in Petri dish. The DPS film was then placed on the HPS film by manipulating the coated silicon substrates under the DPS film and lifting to form the bilayer. A batch of samples was prepared sequentially, using clean water and rinsing the Petri dish between samples.

The batch of specimens was dried in a vacuum oven at room temperature for at least 24 h to remove water trapped between the layers. The samples were heated in a Mettler hot stage at 125 °C for various lengths of time to promote interdiffusion. The final step was to coat a batch of samples simultaneously with 200 Å of Au in order to prevent charging during SIMS experiments. The Au coating technique employed here is the same one used to coat samples for SEM observation.

Testing. A Cameca IMS 3f secondary ion mass spectrometer was used to depth profile the bilayers. The geometry in the SIMS apparatus for testing samples is shown in Figure 4. The incoming primary beam of about 60-μm diameter was rastered over a 500 μm × 500 μm area. Secondary ions were produced over the entire rastered area but a mechanical aperture was used to monitor only a 60-μm circular area in the center of the crater. This elimintated artifacts, such as sputtering from crater walls, that would adversely affect measurement of the depth profile.

The primary beam was Cs^+ with an accelerating voltage of +12.61 kV maintained at a current of 212 nA. The sample was maintained at a constant bias of +4.5 kV. The secondary currents of D^+ and H^+ were the measured quantities. Since the sample had a positive bias, the relative accelerating voltage for the Cs^+ ion was the difference between these voltages, 8.11 kV.

Positive carbon secondary current was measured to monitor the stability of the profile. After steady-state sputtering was achieved, a constant C^+ current indicates that the testing is

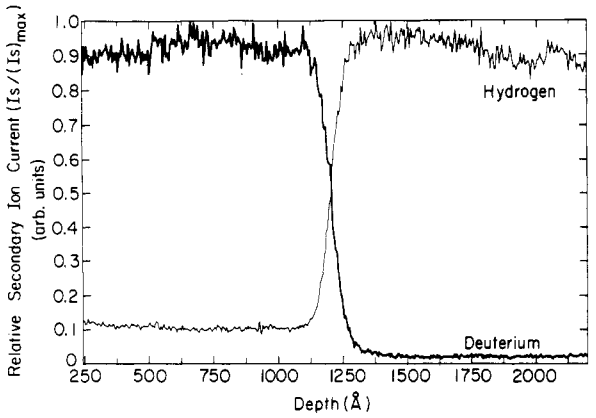

Figure 6. Depth profile for a sharp interface for 111K DPS/93K HPS sample. Abscissa has been converted to a real depth scale for hydrogen and deuterium.

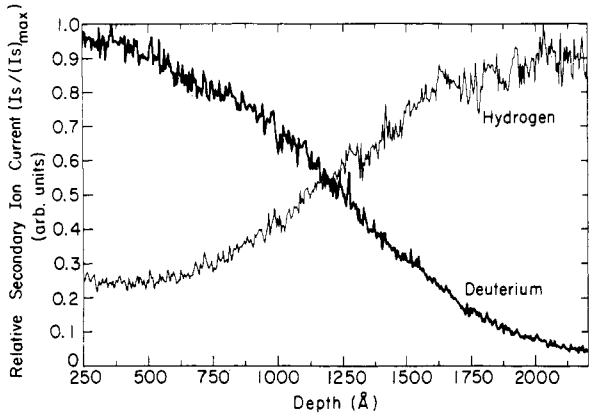

Figure 7. Highly diffused depth profile for hydrogen and deuterium at a DPS/HPS interface. The diffusion couple of 111K DPS/93K HPS was heated at 125 °C for 14 400 s.

proceeding smoothly. The current intensity was plotted in real time on a log intensity versus channel number plot as shown in Figure 5. After testing, the channel (time) scale was converted to a real depth scale by measuring the sample crater depth using a stylus technique.

Results and Discussion

Figures 6 and 7 are depth profiles for a sharp interface and highly diffused couple, respectively. The ordinate was converted to a relative secondary ion current ($I_s/(I_s)_{max}$) and the abscissa was converted to a real depth scale. The carbon secondary ion current was removed because it was only used to monitor the profile during data acquisition as shown in Figure 5. The depth scales in Figures 6 and 7 start at 250 Å in order to remove the transition region needed to establish steady-state sputtering. This region can be safely neglected since it is far from the interface.

Profile Analysis. The profile for the highly diffused couple was analyzed by the Grube method. This approach assumes that the diffusivity coefficient is a weak function of composition.[16] This permits Fick's second law to be written as

$$\frac{\partial c}{\partial t} = \tilde{D}\frac{\partial^2 c}{\partial x^2} \tag{1}$$

where the diffusion coefficient, $\tilde{D}$, is now a constant. The distance from the interface and the concentration at that point are denoted by x and c, respectively. The time for annealing is denoted as t.

This differential equation is then solved for the boundary conditions of a diffusion couple consisting of two semiinfinite films. The result is

$$c = \left[\frac{c_0}{2}\left[1 - \text{erf}\left(\frac{x}{2(\tilde{D}t)^{1/2}}\right)\right]\right] \tag{2}$$

where c_0 is the bulk concentration. Solving for $\tilde{D}$ gives

$$\tilde{D} = \frac{x^2}{4t[\text{erf}^{-1}(1 - 2c/c_0)]^2} \tag{3}$$

Values for the inverse error function were found in standard mathematical tables.

To measure a diffusion distance, an interface must first be established. As a first step, a best-fit line is drawn through the deuterium signal in Figure 7. A horizontal line is drawn parallel to the x-axis at a point halfway between the upper and lower deuterium plateaus. The interface (vertical line) is located at the point where this horizontal line intersects the deuterium signal. This interface is the new datum for distance with positive distances measured to the right and negative distances measured to the left. The point where the upper deuterium plateau intersects the ordinate axis is taken to be c_0. Values for x and c are measured directly from this diffusion profile and used to find $\tilde{D}$ from eq 3.

The value for $\tilde{D}$ found by this method was found to be 5.6×10^{-16} cm^2/s. FRES analysis of a $\bar{M}_w$ = 110K DPS/110K HPS couple healed at 125 °C gives a $\tilde{D}$ value of 3.5×10^{-16} cm^2/s.[1] The small difference in the HPS molecular weight between the SIMS and FRES experiments may account for the slightly larger $\tilde{D}$ for the SIMS experiment since $\tilde{D} \sim M^{-2}$. A highly diffused couple was needed to find $\tilde{D}$ for two reasons: cascade mixing and lack of adhesion. The measured profile (Figure 3a) is a convolution of the true profile and the resolution function. The resolution function is a constant and has a finite width characterized by Δz. The effects of Δz are small when $x \gg \Delta z$. However, deconvolution of measured profiles will be necessary to measure $\tilde{D}$ accurately at short healing times and diffusion distances of the order of Δz.

Many specimens were analyzed in this study. Absence of noticeable diffusion on occassion was attributed to lack of adhesion between the DPS and HPS layers. Diffusion was observed only when long healing times were used. The diffusion time includes time for adhesion and time for diffusion. At long diffusion times, the time needed to start the diffusion process will be a small fraction of the total.

The depth resolution was found to be 138 Å by using the sharp interface profile in Figure 6. Table I compares the depth resolution for several techniques.[3,4] SIMS has a depth resolution comparable to that of SANS with the added advantage of direct depth profile measurement. The program TRIM 86 (transport of ions in matter) was used to model cascade mixing of a +8 kV Cs^+ ion impacting an amorphous carbon target. The stopping power of the polymer sample is due mostly to the carbon. Hydrogen and deuterium do not contribute significantly and were therefore neglected in the model. The primary ion range was found to be 105 Å, which would account for a major portion of Δz. It is quite reasonable to attribute the remaining portion of Δz to surface roughness and instrument parameters. Thus, the intrinsic resolution of the SIMS

Table I
Depth Resolution for Several Techniques

exptl technique	Δz	exptl technique	Δz
SIMS	100–150 Å	FRES	1100 Å
SANS	100–300 Å	IR scanning	100 μm

technique is expected to be closer to 100 Å. The latter result is in agreement with SIMS analysis of polystyrene–poly(methyl methacrylate) diblock copolymers by Coulon et al.[20]

Summary and Outlook

The interdiffusion coefficient for a 111K DPS/93K HPS bilayer specimen healed at 125 °C was found to be 5.6×10^{-16} cm^2/s, in close agreement with FRES results. SIMS combines excellent depth resolution, Δz = 138 Å, with high sensitivity to hydrogen and deuterium. SIMS also has the advantage of direct depth profile measurement.

Measurement of diffusion at short times will require deconvolution of the measured profiles as well as a method for enhancing adhesion between the sample layers. Future work will include investigation of molecular weight effects on polymer diffusion. Correlated motion effects for high molecular weights will also be examined in future experiments and compared with results obtained with neutron specular reflectance techniques.[21]

Acknowledgment. This work was supported by the National Science Foundation under MRL Grant DMR-86-12860. This work made use of facilities in the Center for Microanalysis of Materials at the University of Illinois at Urbana–Champaign. The Center for Microanalysis of Materials is supported by the National Science Foundation under MRL Grant DMR-86-12860 and the Department of Energy under Grant DE-AC02-76ERD1198. We also thank Dr. Chris Loxton and Judy Baker for many useful discussions and technical assistance and Professor E. J. Kramer, Cornell University, for his suggestions on sample preparation techniques.

Registry No. PS, 9003-53-6.

References and Notes

(1) Green, P. F.; Mills, P. J.; Palstrom, C. J.; Mayer, J. W.; Kramer, E. J. *Phys. Rev. Lett.* **1984**, *53*, 2145.
(2) Mills, P. J.; Green, P. F.; Plamstrøm, C. J.; Mayer, J. W.; Kramer, E. J. *Appl. Phys. Lett.* **1984**, *45*,(9), 957.
(3) Klein, J.; Briscoe, B. J. *Proc. R. Soc. London* **1979**, *53*, A365.
(4) Klein, J.; Fletcher, D.; Fetters, L. J. *Nature (London)* **1983**, *304*, 526.
(5) Smith, B. A.; Samulski, E. T.; Yu, L. P.; Winnik, M. A. *Phys. Rev. Lett.* **1984**, *15*, 45.
(6) Bartels, C. R.; Graessley, W. W.; Crist, B. *J. Polym. Sci., Polym. Lett. Ed.* **1983**, *21*, 495.
(7) Summerfield, G. C.; Ullman, R. *Macromolecules* **1987**, *20*, 401.
(8) Briggs, D.; Wootton, A. B. *Surf. Interface Anal.* **1982**, *4*(3), 109.
(9) Briggs, D. *Surf. Interface Anal.* **1986**, *9*, 391.
(10) Valenty, S. J.; Chera, J. J.; Olson, D. R.; Webb, K. K.; Smith, G. A.; Katz, W. *J. Am. Chem. Soc.* **1984**, *106*, 6155.
(11) DiBenedetto, A. T.; Scola, D. A. *J. Colloid Interface Sci.* **1978**, *64*, 480.
(12) Benninghoven, A.; Rudenaur, F. G.; Werner, H. W. *Secondary Ion Mass Spectroscopy, Chemical Analysis Series*; John Wiley: New York, 1987; Vol. 86.
(13) Magee, C. W.; Honig, R. E. *Surf. Interface Anal.* **1982**, *4*(2), 35.
(14) Katz, W.; Newman, J. G. *MRS Bull.* **1987**, *12*(6), 40.
(15) Chadderton, L. T. *Radiation Damage in Crystals*; Barnes and Noble: New York, 1965.
(16) Reed-Hill, R. E. *Physical Metallurgy Principles*, 2nd ed.; Litten Educational; Brooks/Cole Engineering Division: Monterey, CA; 1973.
(17) Green, P. F.; Kramer, E. J. *Macromolecules* **1986**, *19*, 1108.
(18) Binder, K.; Sillescue, H. *Encyclopedia of Polymer Science and Engineering*; John Wiley: New York, in press.
(19) Green, P. F.; Doyle, B. L. *Phys. Rev. Lett.* **1986**, *57*(19), 2407.
(20) Coulon, G.; Russell, T. P.; Deline, V. R.; Green, P. F. *Macromolecules*, in press.
(21) Russell, T. P.; Karim, A.; Mansour, A.; Felcher, G. P. *Macromolecules* **1988**, *21*, 1890.

Raman Spectroscopic Study of the Ionization of Polyelectrolytes. 1. Poly(styrenesulfonic acid) and Poly(ethylenesulfonic acid)

Naoki Tanaka, Hiromi Kitano, and Norio Ise*

Department of Polymer Chemistry, Kyoto University, Kyoto, Japan.
Received September 6, 1988

ABSTRACT: The dissociation behavior of polyelectrolytes such as poly(styrenesulfonic acid) and poly(ethylenesulfonic acid) was examined in aqueous solutions by using laser Raman spectroscopy. These polymeric acids are not completely dissociated: the macroions had a smaller degree of dissociation than the corresponding low molecular weight compounds. The degree of dissociation decreases with increasing concentration of macroions.

Since Kern observed the marked nonideality of polyelectrolyte solutions in terms of the osmotic pressure and single-ion activity coefficients of counterions,[1,2] the association phenomena of couterions with macroions have been one of the central topics for experimentalists and theoreticians working on polyelectrolyte solutions. Unfortunately, however, the exact nature of the interaction between counterions and macroions is still not fully understood. Even some of the conclusions concerning the degree of dissociation of the ionizable groups have varied; for example, Lapanje and Rice[3] stated that poly(styrenesulfonate) is fully dissociated on the basis of the agreement between the Raman spectra of the polymer and its low molecular weight homologue (ethylbenzenesulfonic acid). However, the dissociation of another homologue, *p*-toluenesulfonic acid, was found to be incomplete by Dinius and Choppin[4] using NMR spectroscopy and by Bonner and Torres[5] using Raman spectroscopy. The Raman effect is the reflection of a change in the finite electron density at the bond; in general, purely ionic or ion dipole bonding does not give rise to a Raman band characteristic of the bond.[6] Therefore Raman spectroscopy can be used to measure the state of "true" dissociation in a polyelectrolyte solution. In the present paper, we were interested in studying the reason for the discrepancy mentioned above and also in studying the state of dissociation of poly(styrenesulfonic acid) by using this technique. The state of dissociation of polyacrylate has been previously studied by this method.[7]

Experimental Section

Materials. Sodium poly(styrenesulfonate)s (NaPSS, $\bar{M}_w$ 4000, 16 000, 65 000, and 100 000; $\bar{M}_w/\bar{M}_n$ 1.04–1.06) and sodium poly-

* To whom correspondence should be addressed.

0024-9297/89/2222-2652$01.50/0